AIChE WILEY InterScience DISCOVER SOMETHING GREAT

Thermodynamic Properties of THF + CO_2 Hydrates in Relation with Refrigeration Applications

M. C. Martínez
Cemagref-GPAN, Parc de Tourvoie BP 44, 92163 Antony Cedex, France

D. Dalmazzone and W. Fürst
ENSTA-UCP, 32 bd Victor, 75015 Paris, France

A. Delahaye and L. Fournaison
Cemagref-GPAN, Parc de Tourvoie BP 44, 92163 Antony Cedex, France

DOI 10.1002/aic.11455
Published online February 29, 2008 in Wiley InterScience (www.interscience.wiley.com).

Clathrate hydrate slurries are promising systems in the field of cold distribution. In this work, the L_w-H-V equilibrium conditions, the dissociation enthalpy, and the CO_2 hydration number of a clathrate hydrate formed from THF/CO_2/water mixtures were studied, using a DSC method. For equilibrium condition determination, THF concentration was varied from 1.0 to 16.0 wt % and CO_2 partial pressure range was 0.2 to 2.0 MPa. For enthalpy measurements, THF concentration was fixed at 19 wt % and CO_2 partial pressure investigated from 0.2 to 2.0 MPa. Experimental equilibrium temperatures and enthalpy values were in good agreement with the results of a model combining the van der Waals and Platteeuw approach with the RKS equation of state associated to a MHV2 mixing rule and UNIFAC model. Equilibrium conditions and dissociation enthalpy show that THF + CO_2 hydrate slurries are promising mixtures for refrigeration application. © 2008 American Institute of Chemical Engineers *AIChE J,* 54: 1088–1095, 2008

Keywords: hydrates, CO_2, THF, DSC, dissociation enthalpy

Introduction

Cold production is not only highly energy consuming but it also uses greenhouse-effect refrigerants like HFC. To reduce the quantity of traditional refrigerants, a secondary circuit may be used for cold distribution. The primary circuit using the traditional refrigerant is then confined and minimized, and the secondary circuit distributes cold using alternative fluids. These can be two-phase refrigerants (solid–liquid), called phase-change materials, which are more energy efficient than single-phase refrigerants because of the latent heat of fusion of the solid.

Clathrate hydrate slurries are promising systems in the field of cold distribution and storage as phase-change materials. These crystalline solid compounds are formed by hydrogen-bonded water structure, different from that of ice, stabilized by the presence of "guest" molecules of suitable size and shape inside the cavities formed by the water molecules. Guest molecules interact with the water host molecules through van der Waals forces. The melting temperatures of some clathrate hydrates are consistent with the temperatures needed in applications such as air conditioning (from 279.15 to 285.15 K) or conservation and transport of temperature-sensitive materials that must not

Correspondence concerning this article should be addressed to M. C. Martínez at carmen.martinez@cemagref.fr.

© 2008 American Institute of Chemical Engineers

freeze such as some vaccines.[1] Furthermore, the heat of dissociation of some clathrate hydrates is higher than that of other phase change materials with melting temperatures adapted to these applications, like hydrated salts, paraffin waxes, or fatty acids (between 142 and 253 kJ kg^{-1} at melting temperature between 281 and 286.45 K, as reported in the review of Zalba et al.[2]).

Hydrates formed from gases have been extensively studied because of their importance in the petroleum industry especially because they can plug pipelines during the transport of natural gas or petroleum. But some liquid substances completely miscible with liquid water can also form clathrate hydrates, like liquid cyclic ethers (THF, 1,4-dioxan or ethylene oxide). THF forms a type II clathrate hydrate at atmospheric pressure. It is usually called clathrate hydrate stabilizer because with some guest molecules it can generate a mixed hydrate at a lower pressure than in the case of hydrates generated without THF. Various authors have studied this effect with different guest molecules in various fields, like Seo et al.[3] for CO_2 separation from power plant flue gas (N_2-CO_2-hydrate), Hashimoto et al.[4] for H_2 storage (H_2-CO_2-hydrate), or Delahaye et al.[5] for the use of hydrate slurries as secondary refrigerant (CO_2 hydrate). In these cases the mixed hydrate has a type II structure, THF occupying the large cavities and the other molecules being logged into the small ones.[4,6]

In a previous article,[5] (Lw-H-V) equilibrium conditions for mixed CO_2 + THF hydrate were determined using differential scanning calorimetry (DSC) experiments and represented using an equation of state for the liquid phase and the van der Waals and Platteeuw[7] model for the hydrate phase. Some values of the enthalpies of hydrate dissociation were also estimated applying Clausius Clapeyron equation to the equilibrium data.

The mixed THF + CO_2 hydrate has been proved to have (T, P) stability conditions and heat of dissociation appropriate to its application as secondary refrigerant. The advantage of working with CO_2 containing hydrates is that the hydrate slurry can be generated by direct gas injection into the water solution instead of using mechanical methods, as in the case of ice slurries.

Up to now only estimations of the enthalpy of dissociation for this mixed hydrate were available.[5] In this article we give the results of direct enthalpy measurements performed by calorimetry for systems having a water/THF mole ratio corresponding to stoichiometric THF hydrate. DSC was chosen to generate the various measurements, because it is an efficient technique to study the clathrate hydrates thermodynamics as pointed out by Dalmazzone et al.[8]

Together with hydrate dissociation enthalpy, new equilibrium values have also been obtained in the present study. The new equilibrium measurements are compared with modeling results based on a model combining Van der Waals and Platteeuw[7] approach with a predictive equation of state. As our aim is to consider mainly the heat of hydrate dissociation, we extended the same model to the representation of enthalpy data.

Combination of direct calorimetric enthalpy measurements and Clausius Clapeyron results allowed to estimate the CO_2/water mole ratio in the hydrate and thus the total composition of mixed hydrates at various pressures.

Finally, hydrate dissociation enthalpy reported to the mass of hydrate could be obtained, allowing to compare this value with that of other phase change materials.

Materials and Methods

The DSC device, HP μDSC VII from Setaram, employed for the experimental part is similar to that previously shown by Dalmazzone et al.[9] It can operate at a temperature between 228.15 and 393.15 K. The DSC cells are designed to work up to 40 MPa and their volume is 0.25 cm^3. Because of DSC device characteristics, no stirring can be used. Pressure was measured by a pressure gauge from Bourdon-Sedeme (0–16 MPa, resolution: 0.01 MPa). A reaction calorimeter, C80 from Setaram equipped with in situ mixing vessels was used for the THF in water dissolution enthalpy measurements. The samples were made using freshly distilled and degassed water. Synthesis grade THF from SDS (purity: 99.5 wt %) was distilled on sodium to ensure perfect dryness and was kept under vacuum. CO_2 was provided by Air Liquide (purity: 99.995 vol %).

In this study, mixed THF + CO_2 hydrate has been generated into the DSC cell at constant pressure as is explained hereafter. The sample cell was firstly filled with the proper water-THF solution (25 mg of sample) and then introduced into the calorimeter. A rapid cooling program was then applied to the calorimeter until complete sample crystallization, before purging the vessels three times with CO_2. Previous sample crystallization was necessary to prevent THF elimination during gas purging. At this point, the desired gas pressure was set and kept constant during the subsequent steps of the experiment.

In the presence of THF-water mixtures under CO_2 pressure several solids may appear upon cooling. Two of them are CO_2-containing hydrates, i.e. single CO_2 hydrate and mixed THF + CO_2 hydrate. Two others are CO_2-free phases, i.e. ice and single THF hydrate. At sufficient pressure, the CO_2-containing phases are the more thermodynamically stable phases. However, inserting the poorly soluble CO_2 into the solution requires proper sample stirring. As DSC provides no stirring possibility, we commonly observed the crystallization of ice and THF hydrate in competition with more stable CO_2 and THF + CO_2 hydrates. Even though metastable phases should eventually be changed to stable ones by CO_2 diffusion, this process would require a lot of time. To enhance the rate of phase conversion to CO_2-containing hydrates, successive cooling and warming sequences were applied to the samples in a range of temperatures that was adjusted to successively crystallize and melt ice and single THF hydrate. The maximum temperature of the sequences was kept lower than the dissociation temperature of the more stable solid phases, which were thus allowed to accumulate at each cycle.

Figure 1 shows an example of thermogram recorded at 0.5 MPa of CO_2 and 8 wt % of THF composition. As less stable phases disappear, the areas of crystallization (exothermic) and melting (endothermic) peaks decrease slightly. After running cycles, when the areas of crystallization and melting peaks remain stable, a slower warming program is applied until complete dissociation of the hydrate. Hydrate dissociation step is explained in detail the "Results and Discussion" section.

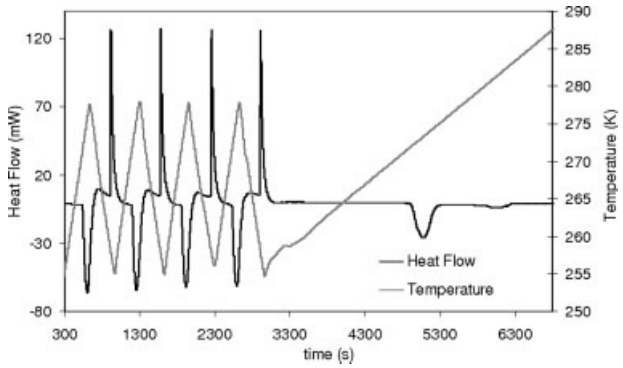

Figure 1. Thermogram obtained for a 8 wt % THF sample at 0.5 MPa of CO_2 with a cyclic temperature program followed by a slower warming program to induce dissociation conditions close to equilibrium.

This multicycle protocol has proven to allow controlling the amount of THF + CO_2 hydrate formed, from very small amounts to a quasi total conversion, by varying the number of cycles.

Modeling of hydrate formation in the water-THF-CO_2 system

In the L_w-H-V system, equilibrium conditions may be expressed through the equality of the chemical potential of all species in all phases. For water, the condition for the hydrate and the liquid phase is given by:

$$\mu_w^{\mathrm{H}} = \mu_w^{\mathrm{L}} \tag{1}$$

Taking as reference value the potential of the phase β Eq. 1 gives:

$$\mu_w^{\mathrm{H}} - \mu_w^{\beta} \equiv \Delta\mu_w^{\mathrm{H}-\beta} = \mu_w^{\mathrm{L}} - \mu_w^{\beta} \equiv \Delta\mu_w^{\mathrm{L}-\beta} \tag{2}$$

where β refers to an hypothetical empty hydrate reference phase.

$\Delta\mu_{\mathrm{w}}{}^{\mathrm{L}-\beta}$ may be expressed as a function of water activity, a_{w}, and the difference between the chemical potential of β and pure liquid water (reference state for water), $\Delta\mu_{\mathrm{w}}{}^{0-\beta}$:

$$\Delta\mu_w^{\mathrm{L}-\beta} = \Delta\mu_w^{0-\beta} + RT\ln a_w \tag{3}$$

$\Delta\mu_{\mathrm{w}}{}^{0-\beta}$ calculation is based on the equation given by Holder et al.[10] considering the contributions expressing the influence of pressure and temperature:

$$\frac{\left(\Delta\mu_w^{\beta-0}\right)_{T,P}}{RT} = \frac{\left(\Delta\mu_w^{\beta-0}\right)_{T_0P=0}}{RT_0} + \int_0^P \frac{\Delta v_w^{\beta-0}}{RT_0}\mathrm{d}P - \int_{T_0}^T \frac{\Delta h_w^{\beta-0}}{RT^2}dT. \tag{4}$$

where

$$\Delta h_w^{\beta-0} = \left(\Delta h_w^{\beta-0}\right)_{T_0} + \int_{T_0}^T \Delta C_{\mathrm{pw}}^{\beta-0}dT \tag{5}$$

The values of parameters $(\Delta\mu_{\mathrm{w}}{}^{\beta-0})_{T_0,P=0}$, $\Delta v_{\mathrm{w}}{}^{\beta-0}$, $\Delta C_{p\mathrm{w}}{}^{\beta-0}$, and $(\Delta h_{\mathrm{w}}{}^{\beta-0})_{T_0}$ relative to structure II are those given in Munck's article[11] and are essentially similar to the parameters published by Parrish and Prausnitz[12]; for the few calculations relative to structure I (without THF) the parameters used are those given by Holder.[10] All these parameters are shown in Table 1. $\Delta\mu_{\mathrm{w}}{}^{\beta-\mathrm{H}}$ is evaluated using the expression of van der Waals and Platteeuw[7]:

$$\Delta\mu_w^{\beta-\mathrm{H}} = -RT\sum_{j=\text{cavities}} v_j \ln\left[1 - \sum_{i=\text{species}} \theta_{ij}\right] \tag{6}$$

where θ_{ij} is the proportion of cavity j occupied by species i according to Eq. 7. Its calculation involves the C_{ij} Langmuir parameters:

$$\theta_{ij} = \frac{C_{ij}\,f_i}{1 + \sum_{\ell=\text{species}} C_{\ell j}\,f_\ell} \tag{7}$$

θ_{ij} is estimated using the temperature dependence Eq. 8 given by Munck et al.[11]:

$$C_{ij} = \frac{A_{ij}}{T}\exp\left(\frac{B_{ij}}{T}\right) \tag{8}$$

A_{ij} and B_{ij} parameter values are those given by Munck et al., except for THF, that only occupies large cavities. The

Table 1. Hydrate Parameters Used for the Calculation of Stability Equilibrium and Enthalpy of Dissociation

Parameters for Eqs. 4 and 5					
Parameter	$\Delta\mu_{\mathrm{w}}^{\beta-0}$ (J mol^{-1})	$\Delta h_{\mathrm{w}}^{\beta-0}$ (J mol^{-1})	$\Delta v_{\mathrm{w}}^{\beta-0}$ (m^3 mol^{-1})	$\Delta C_{P_w}^{\beta-0}$ (J mol^{-1} K^{-1})	
Structure I	1,235*	−4,326*	$4.60 \times 10^{-6\dagger}$	−37.32 + 0.179 (T − 273.15)*	
Structure II	883†	−5,201†	$5.00 \times 10^{-6\dagger}$	−39.16†	
Langmuir parameters for Eq. 8		CO_2		THF	
Compound					
Parameter		A (K Pa^{-1})	B (K^{-1})	A (K Pa^{-1})	B (K)
Structure I	Large cavities	$4.19 \times 10^{-7\dagger}$	2,813†	–	–
	Small cavities	$2.44 \times 10^{-9\dagger}$	3,410†	–	–
Structure II	Large cavities	$8.40 \times 10^{-6\dagger}$	2,025†	6.5972‡	1003.22‡
	Small cavities	$8.34 \times 10^{-10\dagger}$	3,615†	–	–

*Holder et al.[10]
†Munck 1988.[11]
‡Delahaye 2006.[5]

Langmuir parameters for THF were determined in a previous article.[5] All hydrate parameters are given in Table 1.

The water activity a_w and the fugacity f_i of hydrate forming species involved in Eqs. 3 and 7 are calculated using the R-K-S equation of state associated to the MHV2 mixing rule.[13] This mixing rule results in a predictive model when combined to a group contribution G^{ex} model such as Larsen's version of UNIFAC model.[14] The predictive expression for the excess properties used in the calculation of hydrate stability conditions allows to vary the nature of hydrate slurries. The effect resulting from adding new compounds to the system can be predicted to get adapted stability conditions.

The model was validated in three steps. Firstly, the MHV2 + modified UNIFAC predictivity was checked and validated considering the representation of Vapor–Liquid equilibrium data relative to the water-THF system. Secondly, the representation was extended to the stability conditions of single THF hydrate and the THF Langmuir parameter relative to the large cavities of the structure II, $C_{THF\ bII}$, was determined (with 6.5972 K/Pa and 1003.22 K for the parameters $A_{THF\ bII}$ and $B_{THF\ bII}$ in Eq. 8). Finally, a direct extension of the modeling was applied to the water-THF-CO_2 system. Munck's values for A_{ij} and B_{ij} in Eq. 8 were chosen for $C_{CO_2 j}$ calculation.

This model was also used to calculate the hydrate dissociation enthalpy. It was assumed that the main contribution comes from the water molecules. The difference between the partial molar enthalpy for water in the liquid phase and in the hydrate one is calculated by:

$$\frac{\Delta \bar{h}_w^{H-L}}{T^2} = \frac{\partial \frac{\Delta \mu_w^{L-\beta}}{T}}{\partial T} - \frac{\partial \frac{\Delta \mu_w^{H-\beta}}{T}}{\partial T} \tag{9}$$

where the chemical potential variations are calculated from Eqs. 4–8. In these calculations, it is assumed that the contributions of temperature effect on the CO_2 and THF fugacity as well as on water activity a_w are small if compared to the heat of water phase change. Hence the corresponding contributions were neglected.

The validity of these assumptions will be checked by comparing the calculated values with the experimental ones.

Results and Discussion

L_w-H-V equilibrium conditions

Several new determinations were carried out at CO_2 pressures of 0.2, 0.5, 1.0, and 2.0 MPa and for THF mass fractions of 1, 4, 8, 12, 16 wt %, representing an excess of water with respect to the stoichiometric THF hydrate composition of 19.07 wt %. Heat flow evolution recorded by the DSC device upon warming at constant pressure showed two types of endothermic signals. Invariant-temperature peaks, according to the rule of phases, denoted the existence of two solid phases in equilibrium with the vapor and a constant composition liquid phase. These signals were thus attributed to the melting of eutectic mixtures composed of one THF-containing hydrate (either single THF hydrate or mixed THF + CO_2 hydrate) and one THF-free phase (either single CO_2 hydrate or ice). Progressive peaks marked the melting of the single phase remaining after the end of eutectic melting, in equilibrium with the vapor and the variable composition solution. An example of thermogram corresponding to dissociation is shown in Figure 2.

Both kinds of peak were used to determine the corresponding equilibrium temperature: eutectic melting temperature for the first kind, temperature limit of hydrate stability for the second one. A slow warming rate (1.0 K/min) was used for hydrate dissociation, so the system is considered to be very close to thermal equilibrium during the whole process. Then, the temperature corresponding to the end of the melting peak may be assumed to represent the thermodynamic limit of stability of the hydrate in the solution. The L_w-H-V equilibrium temperatures provided by the DSC experiments and the model were compared for the same conditions and illustrated in Figure 3.

The experiments showed that L_w-H-V equilibrium temperatures for mixed THF + CO_2 hydrate increase with CO_2 pressure and THF concentration. Model predictions agree with this result. From 0.2 till 1.0 MPa, melting temperature of eutectic mixture (mixed THF + CO_2 hydrate and ice) remains nearly constant, since ice melting point change scarcely with CO_2 pressure variation. Above this pressure, CO_2 hydrate is more stable than ice, as shown by the model prediction and thus, another eutectic involving single CO_2 hydrate and mixed THF + CO_2 hydrate appears. Since total conversion to CO_2-containing hydrates was not reached in these experiments, the remaining water could freeze at low temperature. Then, two constant temperature transformations were observed upon warming: first, the melting of the eutectic made of metastable ice and mixed THF + CO_2 hydrate, followed by the melting of the second eutectic including both CO_2-containing hydrates. Figure 3c shows the second constant temperature transformation appearing around 278 K.

It may be noticed that THF + CO_2 hydrate is formed at a much lower pressure than single CO_2 hydrate. Indeed CO_2 hydrate equilibrium pressure at 280 K is 2.9 MPa[5] and THF + CO_2 hydrate pressure for 10 wt % THF concentration at the same temperature is only 0.2 MPa.

Deviation between experimental and predicted equilibrium temperatures corresponding to CO_2 pressures between 0.2 and 2.0 MPa for THF concentration between 4 and 16 wt % are shown in Figure 4. Except for three values (THF at

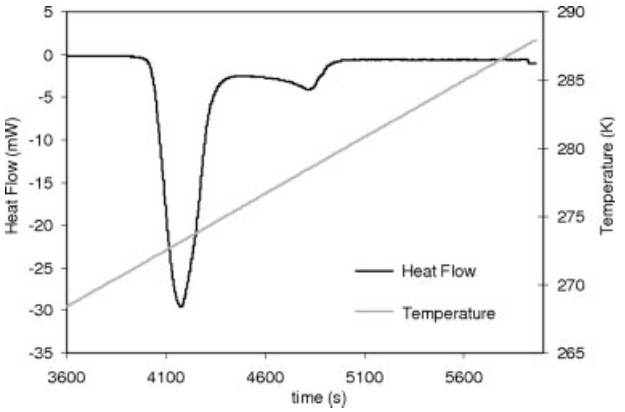

Figure 2. Thermogram showing the dissociation of the hydrate obtained for a 8 wt % THF sample at 0.2 MPa of CO_2.

12 wt % with P_{CO_2} = 0.5 MPa, and THF at 16 wt % with P_{CO_2} = 0.5 and 1.0 MPa), deviation is less than 1.25 K (± 0.6 K over the deviation center). Despite the discrepancies between experimental and modeled results, they can be considered as in good agreement since accuracy in temperature determination with DSC equipment is 0.5 K (progressive transformations).

Nevertheless, a systematic temperature over-estimation is observed. The thermodynamic validity of temperature measurements performed by DSC is mainly based on the assumption that the sample remains thermally homogeneous. This requires properly choosing the warming rate, which must be low enough with respect to the rate of heat transfer within the calorimetric system. To verify whether the experimental conditions could be responsible for the discrepancies observed, we performed additional experiments using a warming rate of +0.2 K/min instead of +1 K/min. The model-experiment deviation at this rate was equivalent to this observed at +1.0 K/min, thus excluding the warming protocol as a source of discrepancies. However, considering that the model use the mixing rule MHV2 and UNIFAC model resulting in a predictive equation of state, the deviations between calculated equilibrium temperatures and the corresponding values obtained from experiment is reasonable (see Figure 4). A better accuracy will be obtained using a model with adjustable parameters.

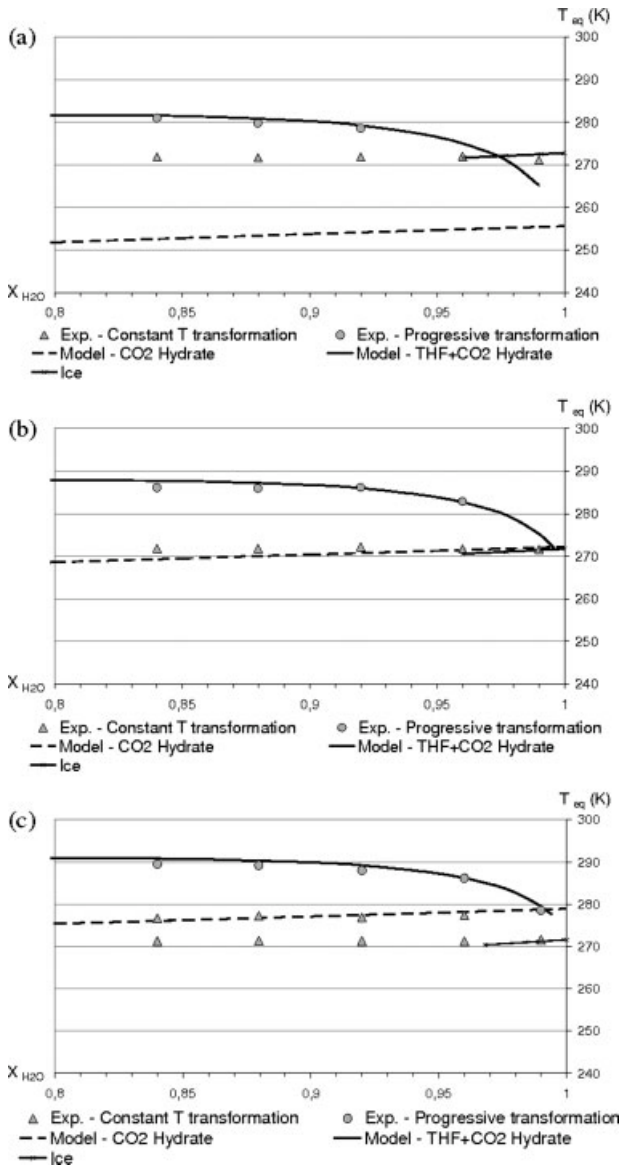

Figure 3. L_w-H-V equilibrium conditions for water-THF-CO_2 system for several CO_2 pressures: (a) 0.2 MPa, (b) 1.0 MPa, and (c) 2.0 MPa.

DSC results (points) show: △ constant temperature transformations (eutectic mixture dissociation) and ○ progressive transformations (THF + CO_2 hydrate progressive dissociation). Modeled results (lines) show hydrate dissociation.

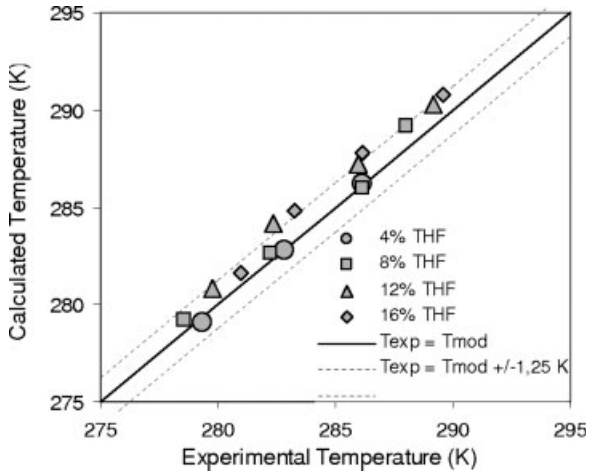

Figure 4. Calculated and experimental L_w-H-V equilibrium temperatures for H_2O-THF-CO_2 system corresponding to CO_2 pressures between 0.2 and 2.0 MPa for various THF concentration between 4 and 16 wt %.

Dissociation enthalpy

The dissociation enthalpy has been obtained after integration of the DSC peak resulting from the evolution of the heat

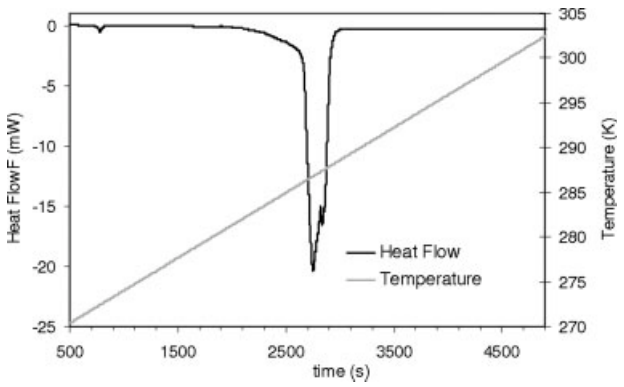

Figure 5. Thermogram showing hydrate dissociation of a sample containing 19 wt % of THF at 1.02 MPa of CO_2 after a long cyclic program.

The first peak correspond to the dissociation of residual eutectic phases and the second one correspond to the mixed hydrate dissociation.

Table 2. THF + CO_2 Hydrate Dissociation Enthalpy for Various CO_2 Pressures: Obtained Experimentally (Exp) and Model Predictions (Model) in Kilojoules per Mole of Water and Their Percentage of Deviation (% Deviation)

P CO_2(MPa)	0.21	0.23	0.37	0.38	0.41	0.52	0.71	0.72	0.74	0.74	0.86	0.95	0.97	1.00	1.02	2.01
Δh (kJ $mol^{-1}_{H_2O}$)																
Model	6.48	6.54	6.73	6.75	6.78	6.90	7.06	7.07	7.08	7.09	7.16	7.22	7.23	7.24	7.25	7.61
DSC	6.33	6.35	6.80	6.55	6.59	6.73	6.74	6.98	7.38	7.12	7.45	7.10	6.88	6.91	7.35	7.40
% Deviation	−2.3	−2.9	1.0	−2.9	−2.8	−2.5	−4.6	−1.3	4.2	0.4	4.0	−1.6	−4.8	−4.7	1.4	−2.8

flow with time during the hydrate dissociation. The experimental procedure was similar to the one described in the section devoted to L_w-H-V equilibrium conditions determination, except that a higher number of temperature cycles (>50) was used to increase the conversion to the more thermodynamically stable phases.

For precise enthalpy measurements, it is essential to know the exact amount of hydrate that has been formed. The formation of solid phases other than the mixed hydrate, such as ice or single CO_2 or THF hydrates, would hinder precise determination of the amount of water involved in the phase of interest. To eliminate such formation, we used THF concentrations very close to the stoichiometry of THF hydrate: 19.07 wt % (17 moles of water of structure II hydrate for each mole of THF). Doing so avoids excess water remain available to form ice or CO_2 hydrate. On the other hand, for higher THF concentrations, excess THF would remain liquid and the decomposition peak would become progressive and thus less convenient for enthalpy measurements. An example of thermogram corresponding to dissociation is shown in Figure 5.

As explained in the "Modeling of hydrate formation in the water-THF-CO_2 system" section, the calculation of the hydrate dissociation enthalpy was made assuming that the main contribution comes from the water molecules neglecting the derivatives of fugacities with respect to temperature as well as on water activity. To get comparable results between DSC experiments and model predictions, DSC results have to be corrected to eliminate the contribution of the enthalpy of dissolution of THF and CO_2 into water. Considering that only a little quantity of CO_2 is present in the liquid phase its contribution was neglected. The enthalpy of dissolution of THF in water, Δh_s, was obtained for 9.2, 12.2, 15.0, and 19.3 wt % THF concentrations at 278.15 and 288.15 K using the C80 calorimeter. Equation 10 gives the correlation obtained between Δh_s (in kilojoules per mole of water) and temperature (in K) for a THF concentration of 19.07 wt %.

$$\Delta h_s = -0.016502 \times T + 4.0928 \tag{10}$$

This value is one-tenth of the dissociation enthalpy and so not negligible. Therefore, experimental results were corrected to eliminate this contribution to the DSC measurement.

Table 2 gives the values obtained experimentally and by the model for the THF + CO_2 hydrate dissociation enthalpy expressed in kilojoules per mole of water, Δh_d, as a function of the CO_2 pressure. Table 2 also gives the relative deviation between experimental and predicted values showing that they are in a good agreement.

Hydration number of CO_2 into the THF + CO_2 hydrate

The hydration number of CO_2 for the THF + CO_2 hydrate, n_{CO_2}, is defined as the water-to-CO_2 mole ratio. This value was determined from the ratio between the hydrate dissociation enthalpy values given in kilojoules per mole of CO_2, $\Delta h'_d$, and the values given in kilojoules per mole of water, Δh_d, as:

$$n_{CO_2} = \frac{\Delta h'_d(\mathrm{kJ/mol}_{CO_2})}{\Delta h_d(\mathrm{kJ/mol}_{H_2O})} \tag{11}$$

The enthalpy values in kilojoules per mole of water were directly determined experimentally and by model predictions, as shown before. As pointed out by Sloan and Fleyfel,[15] the values in kilojoules per mole of CO_2 can be calculated from equilibrium data using the Clausius-Clapeyron equation, Eq. 12.

$$\frac{d\ln P}{d(1/T)} = -\frac{\Delta h'_d}{zR} \tag{12}$$

where $\Delta h'_d$ is expressed in kilojoules per mole of CO_2 consumed by the hydrate formation and z, the compressibility factor, was given by the Nelson-Obert charts[16] for CO_2. The pressure and temperature equilibrium experimental data used were those obtained at 19 wt % of THF when measuring the mixed hydrate dissociation enthalpy. $\Delta h'_d$ values thus obtained are shown in Table 3.

Mixed THF + CO_2 hydrate is supposed to have a type-II hydrate structure, having 16 small cavities (diameter of 3.91 Å) and eight large cavities (diameter of 4.73 Å). Only the small cavities are supposed to be occupied by CO_2 (diameter of 5.12 Å), because large cavities are occupied by THF (diameter of 5.9 Å). If all the small cavities were occupied, the minimum hydration number for the CO_2 would be:

$$n_{CO_2}^{\min} = \frac{136}{16} = 8.5 \tag{13}$$

Table 3. THF + CO_2 Hydrate Dissociation Enthalpy for Various CO_2 Pressures Calculated by the Clausius-Clapeyron Equation Based on Experimental Equilibrium Data (Exp) at 19 wt % of THF in Kilojoules per Mole of CO_2

P CO_2(MPa)	0.21	0.23	0.37	0.38	0.41	0.52	0.71	0.72	0.74	0.74	0.86	0.95	0.97	1.00	1.02	2.01
$\Delta h'$ (kJ $mol_{CO_2}^{-1}$)																
Exp × 10^{-2}	1.70	1.70	1.69	1.69	1.68	1.67	1.65	1.65	1.65	1.65	1.64	1.63	1.63	1.63	1.62	1.52

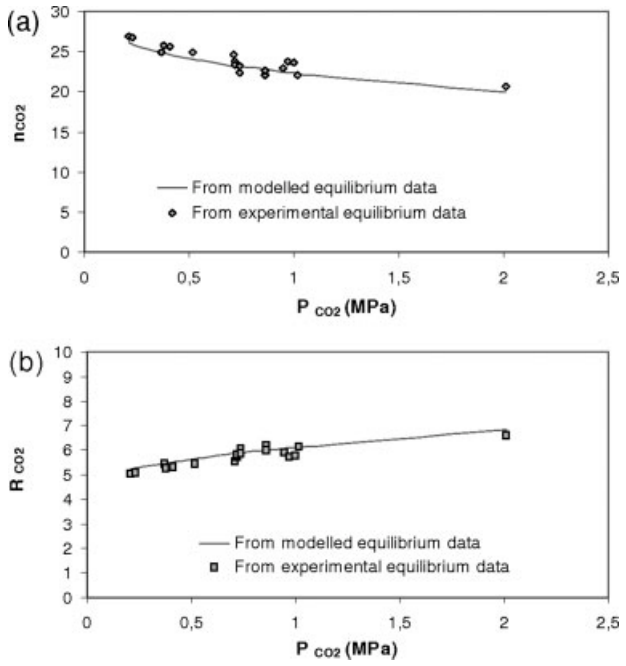

Figure 6. Evolution of (a) the hydration number of CO_2 into the mixed THF + CO_2 hydrate, n_{CO_2}, and (b) the ratio moles of CO_2 per moles of mixed THF + CO_2 hydrate, R_{CO_2}, with pressure for 19 wt % THF concentration.

Values obtained from experimental and model prediction data.

Type-II hydrates have 136 moles of water per mole of hydrate. The number of moles of CO_2 contained in one mole of hydrate, R_{CO_2} can be determined as:

$$R_{CO_2} = \frac{\text{mol CO}_2}{\text{mol hydrate}} = \frac{\Delta h_d(\text{J/mol}_{H_2O})}{\Delta h'_d(\text{J/mol}_{CO_2})} \times \frac{136\,\text{mol}_{H_2O}}{\text{mol}_{\text{hydrate}}} \quad (14)$$

Figure 6 shows the evolution of n_{CO_2} and R_{CO_2} with pressure for 19 wt % THF concentration. As it can be seen, the obtained hydration number for CO_2 is significantly higher than the minimum hydration number shown in Eq. 13.

The maximum R_{CO2} value considering only small cavities to be occupied by CO_2 is 16, so the occupancy of small cavities varies between 32 and 42% as CO_2 pressure increases. Sloan[17] pointed out that typical occupancies of large cavities in natural gas hydrates are greater than 95%, while occupancy of small cavities are usually on the order of 50%. The large CO_2 diameter (5.12 Å of diameter) may justify the low occupancy obtained: small cavities have a diameter of 3.91 Å, a distortion of the structure is necessary to include CO_2 into the small cavities of the hydrate.

The molar weight of the THF + CO_2 hydrate was calculated using the R_{CO2} values obtained, and thus allowed to calculate the dissociation enthalpy in kilojoules per kilogram of hydrate (see Table 4). These values, for the range of CO_2 pressure studied, were lower than those obtained for the CO_2 hydrate (374.3 kJ $kg_{hydrate}^{-1}$ at 273.65 K[18]), but higher than those of the THF hydrate (262.9 kJ $kg_{hydrate}^{-1}$ at 273.65 K[19]).

These values of mixed hydrate enthalpy may seem to differ from those reported by Delahaye et al.[5] where mixed hydrate showed higher dissociation enthalpy than single CO_2 hydrate. Actually, there is no discrepancy, i.e., Delahaye et al. values were directly obtained by the Clausius-Clapeyron equation and so given in kilojoules per mole of CO_2 contained into the hydrate (comparable values to those obtained in the present article and shown in Table 3 for 19 wt % of THF). Single CO_2 hydrate contains 5.738 $mole_{CO_2}/kg_{hydrate}$ and mixed THF + CO_2 hydrate contains from 1.6 $mole_{CO_2}/kg_{hydrate}$ (at 0.2 MPa) to 2.055 $mole_{CO_2}/kg_{hydrate}$ (at 2.1 MPa). The different quantity of CO_2 contained in mixed and single hydrate per mass unit explains that the energetic rate between both of them is not the same when dissociation enthalpy is reported to the mole of CO_2 or to the mass of the whole hydrate.

Conclusion

In the present study, mixed THF + CO_2 hydrate formation conditions and its dissociation enthalpy were experimentally determined on water-THF-CO_2 system using a DSC device. A model combining the van der Waals and Platteeuw approach with the Redlich-Kwong-Soave equation of state associated to a Modified Huron-Vidal (MHV2) mixing rule and UNIFAC model was employed to predict equilibrium temperatures and dissociation enthalpy of the mixed THF + CO_2 hydrate. Phase diagrams for CO_2 pressures between 0.2 and 2.0 MPa and THF concentration between 1 and 16 wt % were then proposed showing eutectic phases composition and its evolution with pressure. Experimental results were compared with modeled predictions and a good agreement was found.

Dissociation enthalpy of THF + CO_2 hydrate per mole of water was also measured by DSC for a THF concentration of 19 wt % and CO_2 pressures from 0.2 to 2.0 MPa. These values were compared with modeled predictions and a good agreement was found, validating the assumptions made in the model. Clausius-Clapeyron equation was used with the equilibrium data obtained at 19 wt % of THF to calculate the dissociation enthalpy of the mixed THF + CO_2 hydrate per mole of CO_2 contained within the hydrate. CO_2 hydration number for the mixed hydrate was then estimated. Finally, dissociation enthalpy per mass of mixed THF + CO_2 hydrate was calculated. This enthalpy study seems to confirm mixed THF + CO_2 hydrate as a suitable solid to be used in the field of cold storage and cold distribution.

Table 4. THF + CO_2 Hydrate Dissociation Enthalpy Based on Experimental Equilibrium Data (Exp) at 19 wt % of THF in Kilojoules per Kilogram of Hydrate

P CO_2 (MPa)	0.21	0.23	0.37	0.38	0.41	0.52	0.71	0.72	0.74	0.74	0.86	0.95	0.97	1.00	1.02	2.01
ΔH (kJ kg^{-1}) Exp $\times 10^{-2}$	2.65	2.66	2.83	2.74	2.75	2.80	2.81	2.90	3.05	2.95	3.08	2.61	2.86	2.87	3.04	3.04

Notation

a_w = activity in water
A_{ij} = Langmuir constant parameter for component i in cavity j (K Pa^{-1})
B_{ij} = Langmuir constant parameter for component i in cavity j (K)
C_{ij} = Langmuir constant for component i in cavity j (1 Pa^{-1})
L_w-H-V = aqueous liquid–hydrate–vapor
f_i = fugacity for component i (Pa)
P = pressure (Pa)
R = universal gas constant (J mol^{-1} K^{-1})
T = temperature (K)
T_{ref} = reference temperature (K)
T_0 = standard temperature (K)
X_{H_2O} = mass fraction of water
z = gas compressibility
n_{CO_2} = hydration number for CO_2 into the THF + CO_2 hydrate (mol_{H_2O} $mol_{CO_2}^{-1}$)
$n_{CO_2}^{min}$ = minimum hydration number for CO_2 into the THF + CO_2 hydrate (mol_{H_2O} $mol_{CO_2}^{-1}$)
R_{CO_2} = mole of CO_2 contained in one mole of THF + CO_2 hydrate (mol_{CO_2} $mol_{hydrate}^{-1}$)

Greek letters

β = theoretical empty hydrate
$\Delta C_{pw}^{\beta-0}$ = heat capacity difference of water between phase β and pure liquid water phase (J mol^{-1} K^{-1})
$\Delta h_w^{\beta-0}$ = molar enthalpy difference of water between β and pure liquid water phases at T_{ref} and zero absolute pressure (J mol^{-1})
$\left(\Delta h_w^{\beta-0}\right)_{T_0}$ = molar enthalpy difference of water between β and pure liquid water phases at temperature T_0 and zero absolute pressure (J mol^{-1})
$\overline{h}_w^H$ = partial molar enthalpy of water in the hydrate phase (J $mol_{H_2O}^{-1}$)
$\Delta \overline{h}_w^{H-\beta}$ = partial molar enthalpy difference of water between hydrate phase and β phase (J $mol_{H_2O}^{-1}$)
Δh_s = THF in water dissolution enthalpy (J $mol_{H_2O}^{-1}$)
Δh_d = THF + CO_2 hydrate dissociation enthalpy (J $mol_{H_2O}^{-1}$)
$\Delta h_d'$ = THF + CO_2 hydrate dissociation enthalpy (J $mol_{CO_2}^{-1}$)
μ_w^H = water chemical potential in hydrate (J mol^{-1})
$\Delta \mu_w^{\beta-L}$ = water chemical potential difference between β and liquid phases (J mol^{-1})
$(\Delta \mu_w^{\beta-0})_{T,P}$ = water chemical potential difference between phase β and pure liquid water at temperature T and at pressure P (J mol^{-1})
$\Delta v_w^{\beta-0}$ = water volume difference between β and pure liquid water phases in standard conditions (m^3 mol^{-1})
v_j = number of type j cavities per water molecule in unit cell
θ_{ij} = fractional occupation of cavity j by component i

Literature Cited

1. Zweig SE. Advances in vaccine stability monitoring technology. *Vaccine*. 2006;24:5977–5985.
2. Zalba B, Marin JM, Cabeza LF, Mehling H. Review on thermal energy storage with phase change: materials, heat transfer analysis and applications. *Appl Therm Eng*. 2003;23:251–283.
3. Seo Y-T, Kang H, Lee H. Experimental determination and thermodynamic modeling of methane and nitrogen hydrates in the presence of THF, propylene oxide, 1,4-dioxane and acetone. *Fluid Phase Equilib*. 2001;189:99–110.
4. Hashimoto S, Murayama S, Sugahara T, Ohgaki K. Phase equilibria for H_2 + CO_2 + tetrahydrofuran + water mixtures containing gas hydrates. *J Chem Eng Data*. 2006;51:1884–1886.
5. Delahaye A, Fournaison L, Marinhas S, Chatti I, Petitet J-P, Dalmazzone D, Fürst W. Effect of THF on equilibrium and dissociation enthalpy of CO_2 hydrates applied to secondary refrigeration. *Ind Eng Chem Res*. 2006;45:391–397.
6. Mak TCW, McMullan RK. Polyhedral clathrate hydrates. X. Structure of the double hydrate of tetrahydrofuran and hydrogen sulfide. *J Chem Phys*. 1965;42:2732–2737.
7. van der Waals JH, Platteeuw JC. Clathrate solutions. *Adv Chem Phys*. 1959;2:1–57.
8. Dalmazzone D, Clausse D, Dalmazzone C, Herzhaft B. The stability of methane hydrates in highly concentrated electrolyte solutions by differential scanning calorimetry and theoretical computation. *Am Mineral*. 2004;89:1183–1191.
9. Dalmazzone C, Hamed N, Clause D, Fouconnier B, Dalmazzone C, Herzhaft B. The use of DSC in the study of the thermodynamics and kinetics of formation of model and gas hydrates. In: Proceedings of the 5th International Conference on Gas Hydrates, Trondheim, Norway, 2005; p 4005.
10. Holder GD, Corbin G, Papadopoulos KD. Thermodynamic and molecular properties of gas hydrates from mixtures containing methane, argon, and krypton. *Ind Eng Chem Fundam*. 1980;19:282–286.
11. Munck J, Skjold-Jorgensen S, Rasmussen P. Computation of the formation of gas hydrate. *Chem Eng Sci*. 1988;43:2661–2667.
12. Parrish WR, Prausnitz JM. Dissociation pressures of gas hydrates formed by gas-mixtures. *Ind Eng Chem Process Des Dev*. 1972;11:26–35.
13. Dahl S, Fredenslund A, Rasmussen P. The MHV2 model: a UNIFAC-based equation of state model for prediction of gas solubility and vapor-liquid equilibria at low and high pressures. *Ind Eng Chem Res*. 1991;30:1936–1945.
14. Larsen BL, Rasmussen P, Fredenslund A. A modified UNIFAC group-contribution model for prediction of phase equilibria and heats of mixing. *Ind Eng Chem Res*. 1987;26:2274–2286.
15. Sloan ED, Fleyfel F. Hydrate dissociation enthalpy and guest size. *Fluid Phase Equilib*. 1992;76:123–140.
16. Çengel YA, Boles MA. *Thermodynamics: An Engineering Approach*, 4th ed. Boston: McGraw-Hill, 2002.
17. Sloan ED. *Clathrate Hydrates of Natural Gases*, 2nd ed. New York: Marcel Dekker, 1998.
18. Kang S-P, Lee H, Ryu B-J. Enthalpies of dissociation of clathrate hydrates of carbon dioxide, nitrogen, (carbon dioxide + nitrogen), and (carbon dioxide + nitrogen + tetrahydrofuran). *J Chem Thermodyn*. 2001;33:513–521.
19. Handa YP, Hawkins RE, Murray JJ. Calibration and testing of a Tian-Calvet heat-flow calorimeter. Enthalpies of fusion and heat capacities for ice and tetrahydrofuran hydrate in the range 85 to 270K. *J Chem Thermodyn*. 1984;16:623–632.

Manuscript received Sept. 25, 2007, and revision received Dec. 7, 2007.